Neuropsychologia 222 (2026) 109351

Contents lists available at ScienceDirect

Neuropsychologia

journal homepage: www.elsevier.com/locate/neuropsychologia

Bayesian cue combination best predicts straight-line distance estimation with translated visual landmarks

Abhilasha Vishwanath [a,b,*], Matthew F. Watson [a], Melanie K. Gin [a], Donnette C. Markham [a], Yinqi Huang [c], Yu K. Du [a], Arne Ekstrom [a,b,1], Robert C. Wilson [c,1]

[a] Psychology Department, The University of Arizona, Tucson, AZ, United States
[b] McKnight Brain Institute, The University of Arizona, Tucson, AZ, United States
[c] School of Psychology, Georgia Institute of Technology, Atlanta, GA, United States

ARTICLE INFO

Dataset link: TranslationModeling (Original data)

Keywords:
Spatial navigation
Path integration
Landmark navigation
Computational modeling
Cue combination
Bayesian integration

ABSTRACT

Navigation requires the ability to update and track one's location and course from available multisensory information. Multisensory input comes in two prominent forms: body-based idiothetic cues and visual allothetic cues, usually from visual landmarks. Yet, how these two streams of information are integrated remains unresolved. In this study, we used a highly controlled straight-line distance estimation task in immersive virtual reality to investigate how idiothetic and allothetic spatial cues are integrated. In our experiment, participants reproduced a walked distance in the dark (path integration), with some trials involving misleading visual feedback showing a translated virtual room with an offset of up to 1.5 m from the true distance. We used computational modeling to determine the effect of visual feedback offset on the distance participants walked. We modelled participants' performance on the task with three distinct models involving path integration, landmark navigation, and integrating landmark feedback based on the uncertainty of the participant. The model results showed that the behavior of most participants (n = 24) was best predicted by a Bayesian cue combination model that involved averaging the two spatial cues according to their perceived level of uncertainty. Our data showed considerable individual differences in the uncertainty estimates of participants, which spanned almost uniformly from pure path integration (ignoring the visual cue) to pure landmark navigation (ignoring path integration estimate). Taken together these findings provide evidence in favor of Bayesian cue combination strategy in distance reproduction with individual differences in navigation behavior dictated by perceived level of uncertainty.

1. Introduction

Navigation is a complex behavior that many species depend on for daily survival. The ability to navigate requires evaluating multisensory information to transverse and remember spaces and distances in one's environment. The two prominent forms of multisensory inputs are idiothetic cues, which includes systems informing body-based cues such as proprioceptive, vestibular, and motor systems, as well as optic flow, and allothetic cues, which can be anchor points in the environment like visual landmarks. Integration of multiple cues is likely to yield better estimations of position during navigation given that any single cue presents an incomplete picture and is often error prone. Yet, how we integrate sensory cues in different situations has multiple possibilities and depends on the complexity of the behavior/task. In our study, we use a one-dimensional distance estimation task in an immersive virtual reality environment to delineate the use of idiothetic and allothetic cues.

Navigation using only idiothetic cues, for example navigating in the dark, is called path integration. The ever-present nature of body-based cues makes it an important source of information that is likely used continuously in human navigation. However, our internal path integration estimates are prone to inaccuracies due to biased and noisy sensory information. Specifically, in distance estimation, path integration produces biases based on systematic over- and under-estimation (Chrastil and Warren, 2021; Harootonian et al., 2020), as well as prior

This article is part of a special issue entitled: Maps in the Brain published in Neuropsychologia.

* Corresponding author. Psychology Department, The University of Arizona, Tucson, AZ, United States.
E-mail address: avishwanath@arizona.edu (A. Vishwanath).

[1] These authors contributed equally.

https://doi.org/10.1016/j.neuropsychologia.2025.109351
Received 14 May 2025; Received in revised form 3 October 2025; Accepted 20 December 2025
Available online 22 December 2025

experience and range effects (Petzschner and Glasauer, 2011; Teghtsoonian and Teghtsoonian, 1978). The accumulation of errors in the path integration process usually scales with the magnitude or distance length in a Weber-Fechner and Steven's power law like behavior (Harootonian et al., 2020; Petzschner and Glasauer, 2011).

Navigation using only allothetic cues such as visual landmarks is called map or landmark navigation (Waller and Nadel, 2013). Decoupling visual landmarks from idiothetic body-based cues can allow the study of pure landmark navigation, which can be done in virtual environments where visual landmarks can be dynamically manipulated (Nardini et al., 2008; Sjolund et al., 2018). As participants can use either beaconing (navigating towards a visible landmark) or allocentric strategies, even with limited body movements, it is also clear that they can use visual-based landmark information nearly exclusively in some situations (Huffman and Ekstrom, 2019). Yet, when and how participant's path integration and landmark information are combined remains unclear.

To navigate effectively, it is important to use both path integration and visual landmarks as neither provide the complete information in isolation. One approach for integrating noisy path integration and possibly misleading visual landmarks is combining or averaging the estimates from both cues known as the cue combination strategy. In 'cue combination' models the distance or location is computed from combining path integration and landmark navigation cues. The cues are combined with the average biased towards path integration or landmark cue in a probabilistic distribution using Bayes' rule (Knill and Pouget, 2004; McNamara and Chen, 2022). Thus, the averaging process is often assumed to be Bayesian, with the weighted average based on the uncertainty or reliability of the cues (Deneve and Pouget, 2004; Ma, 2012). This is sometimes thought to be the optimal Bayesian cue combination behavior that is supported in some studies (Chen et al., 2017; Nardini et al., 2008; Whishaw and Tomie, 1997; Xu et al., 2017). A recent study by Chen et al. (2025), showed that a Bayesian casual inference model outperformed a non-Bayesian model for visual conflict resolution of perceived distance using desktop VR. It is crucial to understand if the Bayesian cue combination model prevails in reconciling landmark uncertainty in a fully immersive VR design.

Alternatively, another approach to cue integration is a hybrid or cue competition model. In this model, the sensory cues compete such that one cue is favored over the other based on certain factors like proximity of two visual cues (Chen et al., 2017; Deery and Commins, 2023) or probabilistic uncertainty between two different sensory cues (Harootonian et al., 2022). For instance, a lower uncertainty of path integration compared to visual landmark cues determines the use of path integration for that situation and vice versa. In contrast to these cue integration approaches, single-cue strategies like 'pure' path integration (using just internal body-based cues and ignoring allothetic information) and 'pure' landmark navigation (estimating position using landmarks in the environment and ignoring path integration estimates) are another possibility. Better understanding these varying strategies can provide insight into how the brain processes and utilizes multisensory cues in a goal-directed behavior like navigation. Most studies investigating these strategy differences use a more complex homing or triangle completion task (Chen et al., 2017; Chrastil and Warren, 2021; Fujita et al., 1993; Kessler et al., 2024; Mou and Zhang, 2014; Nardini et al., 2008; Scherer et al., 2024; Zhao and Warren, 2015). Typically, in a triangle completion task, participants are guided along two sides of a triangle and then asked to navigate the third leg back to their starting location relying only on path integration or with visual landmark cues. This task requires participants to keep track of both direction and distance to complete the triangle making it harder to disentangle distance and angular estimates. In addition, there is large inter-individual and inter-trial variability across studies (Kessler et al., 2024; Weisberg et al., 2014) due to individual differences in navigation ability (Chrastil et al., 2017; Waller, 2000; Weisberg and Newcombe, 2018) and low level processes, such as differences in inferring distance from haptic and kinesthetic information during locomotion (Ehinger et al., 2014; Schwartz, 1999; Singapogu et al., 2008).

In our previous work, we created a purely angular estimation task called the 'Rotation Task' (Harootonian et al., 2022) to disentangle the direction component. In the Rotation Task, participants encoded up to 360° in an immersive virtual environment while turning around in place. During reproduction of the turned angle, a brief (300 ms) flash of consistent or misleading visual feedback of the room was presented. This way the effect of visual feedback was studied in just angular estimation using cue integration and pure path integration or landmark navigation models. This template was used to create a task that is specific to distance estimation alone.

In our current study, we created a one-dimensional distance estimation task termed the 'Translation Task' to disentangle the linear distance estimation. In this task, participants walked to an encoded goal distance with visual feedback that either matched or mismatched their expectations. Participants then attempted to retrieve the distance they had just encoded by walking it while the room was visible for half the trial. The room position either matched the true position of the room or was translated forward or backward. We used a fully immersive virtual environment to investigate how people combine body-based idiothetic and visual allothetic cues when computing location of straight-line distance. We first investigated the computational properties of this task, via simulation, and used a subset of the models that we could distinguish to investigate human behavior. We modelled the behavior of participants on the Translation Task using Bayesian cue combination and "pure" strategies of path integration and landmark navigation to try to understand how participants might use either landmark information or path integration, or their combination, to retrieve the straight-line path. This also allowed us to look for individual differences (Ishikawa and Montello, 2006; Weisberg et al., 2014) in how the different cues were weighted during retrieval of the straight-line distance.

2. Methods

2.1. Participants

Participants were recruited from the University of Arizona and surrounding area as part of a larger study. Thirty participants (8 male, age range 18–28 years, mean age 20.43 years) were included in the study. Participants were compensated with $20 an hour. All participants provided written informed consent before participating in the study. The study and methods were approved by the Institutional Review Board at the University of Arizona.

2.2. Experiment

The current Translation Task was modified from a previously published Rotation Task (Harootonian et al., 2022). The Translation Task lasted about 2 h and consisted of 160 trials (Fig. 1C). Participants typically completed this task in addition to other tasks (most common, the Rotation Task, not analyzed in this paper). Tasks were counter-balanced between participants.

2.2.1. Apparatus

The task was developed using Landmarks 2.0 framework (Starrett et al., 2021) in Unity 2018.4.11f1 paired with wireless HTV Vive pro headset and controllers (Fig. 1A). All experiments were performed in a ~12m × 5m physical room. The 4 HTC Base Stations used for tracking position were extended to span the size of the physical room. The virtual environment for the Translation Task consisted of a large rectangular (8m × 5m x 5m) virtual room where participants walked back and forth on the red carpet that ran along the center of the virtual room. The virtual room was designed with distinguishable features at either end of the carpet with a bookshelf and windows at one end and a door and bookshelves on the other (Fig. 1B). The features on either side of the

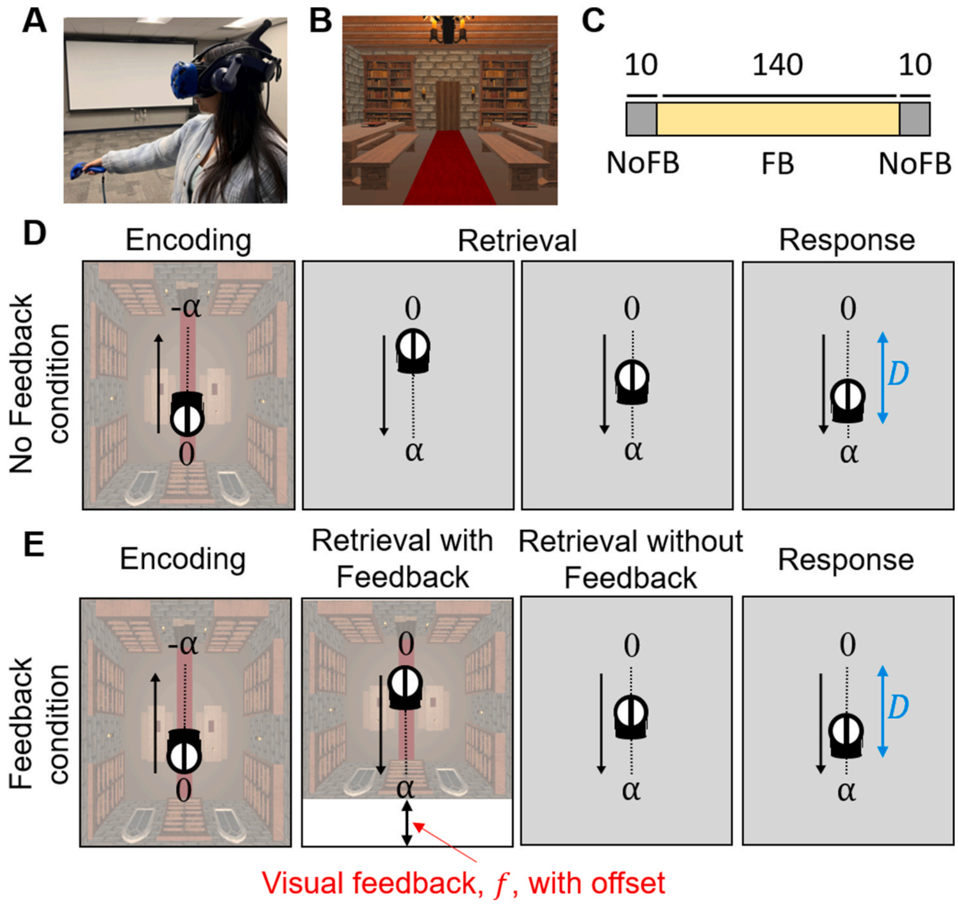

Fig. 1. Translation task procedure. (A) Participant wearing HTC VIVE headset and holding the handheld controllers to perform immersive virtual reality task. (B) Participant view of the virtual room during encoding at the beginning of a trial. (C) Overall participants completed 160 trials of the translation task which consisted of 20 No Feedback (NoFB) trials and 140 trials with Feedback (FB). (D) Trial timeline during the No Feedback condition. Trial starts with participants facing the door and proceeding to walk with full view of the room until distance $-\alpha$ (encoding phase). During the retrieval phase, participants turn around in the dark and walk back to the start/bookshelf, α distance, without visual feedback (grey rectangles) at any point during this phase. Finally, participants respond using the controller to indicate response distance, D. (E) Same as in (D) but for Feedback condition with different retrieval phase. During retrieval, participants receive visual feedback, f, for half the total target distance, α. At this point, the feedback is turned off and participants continue walking without visual feedback.

carpet were identical.

2.2.2. Translation task

On a given trial participants walked with full view of the room until a certain distance of $-\alpha$, ranging between 2 and 7.9 m (encoding phase). During the retrieval phase, participants were asked to walk back to their initial position, termed 'target distance' $+\alpha$ with or without visual feedback (Fig. 1DE). When presented, the visual feedback was a visual rendering of the room either at its "true" or "translated" location. The main outcome measure of the task was the error in distance estimation. This allowed us to investigate how visual feedback affected the walked distance.

Specifically, at the start of a trial participants were guided to a starting position in the dark using a red circle on the virtual floor. The starting position was randomly selected to be at either end of the physical room. Once at the starting position, participants were presented with the full view of the virtual room along its length always facing the door with the bookshelf at their back during the encoding phase. Participants would then walk along the red carpet in the center of the room until the room disappeared at distance $-\alpha$, which was randomly sampled for each trial from a uniform distribution $U(\alpha)$. Participants were then guided in the dark to turn around and face the direction of their starting position using a green circle and arrow on the virtual floor. They were then instructed to walk to their starting position.

During the No Feedback trials (n = 20), participants walked back to their starting position without any visual feedback (Fig. 1D), thus participants could only rely on their estimates from path integration to make their distance estimation.

During the Feedback trials (n = 140), participants were presented with visual feedback, f, at the start of the retrieval phase (Fig. 1E). Participants walked back with visual feedback, i.e., facing the bookshelf with a full view of the room, until they reached the mid-point of the target distance. At this point, the visual feedback disappeared and participants were asked to continue in the dark to get to the target distance if needed. Participants would indicate their response using a button on one of their handheld controllers to record their response distance, D_t.

The visual feedback presented was correct for 20 of the 140 Feedback trials. For the remaining trials, consistent feedback was presented with probability, $\rho = 0.6$, in which the feedback was sampled from a Gaussian distribution centered around the true target distance with a standard deviation of 0.1 m. Inconsistent feedback was presented with probability, $1 - \rho = 0.4$, in which the feedback was sampled from a uniform distribution between − 1.5 to + 1.5 m. When written mathematically, the feedback distance, f was sampled using

$$f \sim \begin{cases} f = \alpha & \text{on 20 trials} \\ N\left(f \middle| \alpha, \sigma_f^2\right) & \text{on remaining trials with probability } \rho = 0.6 \\ U(f| -1.5, 1.5) & \text{on remaining trials with probability } 1-\rho = 0.4 \end{cases} \quad \text{Eq. 1}$$

where $N\left(f \middle| \alpha, \sigma_f^2\right)$ is a Gaussian distribution over f with mean α and standard deviation $\sigma_f = 0.1$ meters. The matching and mismatching visual feedback were randomized for all participants. We removed trials in which participants indicated a response before the end of feedback presentation.

Participants were not informed that the feedback presented could be misleading in order to further encourage incorporation of visual feedback. Participants were prevented from seeing the physical room for the entirety of the experiment so as to ground them in the virtual environment and avoid inference in distance estimation based on the scale of the physical room. Participants were not instructed on a walking pace and were allowed to set their own pace during encoding and retrieval phases.

The current specification for visual feedback presentation and virtual room length was adjusted based on pilot data. First, for participants to exhibit naturalistic path integration variations in distance estimation, i.e., without any visual feedback during retrieval, the length of the virtual room and consequently the physical room were extended to the current dimensions based on initial piloting in a smaller room. The distance response as a function of target distance is shown for all participants (n = 30) during the No Feedback trials (Fig. 2); it is evident that participants are mostly accurate with reasonable variability across trials. Second, visual feedback of the misleading room length was not effective in eliciting error in distance reproduction when the feedback was presented as a brief (300 ms) flash either in the smaller or larger room during piloting. The length of time for visual feedback had to be increased to half the length of the encoding distance to influence distance estimation. Thus, participants had to walk a certain distance with misleading feedback for visual feedback to be incorporated in some fashion. Given the larger physical room, we were able to extend the visual feedback offset (± 1.5 m). Allowing us to investigate the parametric changes and individual differences in the error responses.

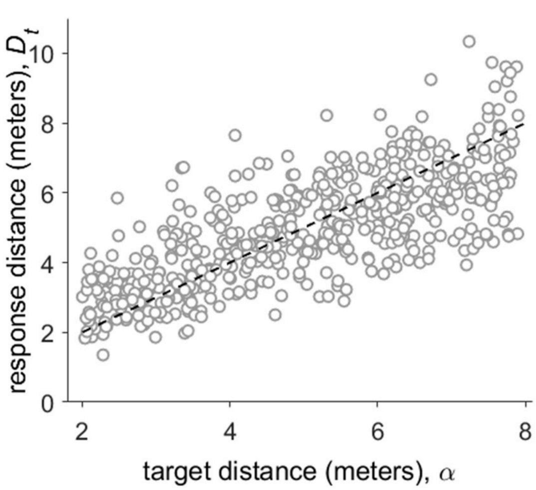

Fig. 2. Relatively accurate path integration in participants during No Feedback trials. Scatter plot showing relationship between target distance, α, and response distance, D_t for all participants (n = 30) for all no feedback trials (n = ~20 each). Dotted line shows perfect linear relationship.

2.3. Models

The models used for the Translation Task were adapted from the models used in the Rotation Task (Harootonian et al., 2022). Three models were built to capture the translation behavior during the retrieval phase of the task and the strategies used for integrating allothetic visual and idiothetic body-based estimates of distance. The encoding phase was not modelled as it did not change across trials or conditions and was performed in the presence of all sensory cues. A glossary of variables is provided to keep track of parameters used in the models (Table 1).

2.3.1. Path integration model

This model assumes that participants rely only on vestibular, proprioceptive, and motor-efferent copy body-based cues to guide their distance. Such a situation is always the case on No Feedback trials as participants have no visual feedback to guide them during retrieval. On the Feedback trials, this model captures behavior if people ignore the visual stimulus.

In this model, we assume that people use path integration to keep track of their distance and stop when their estimated distance matches the remembered target distance. As previously described in (Harootonian et al., 2022), we can therefore breakdown the path integration model into two steps: path integration and target comparison.

2.3.1.1. Path integration. We assume that participants keep track of their location over time, by integrating internal velocity cues (that themselves are computed by integrating internal acceleration cues from the vestibular system and motor commands). Importantly, we assume that the internal velocity cues d_t may not always reflect the true velocity δ_t

$$d_t = \gamma_d \delta_t + \nu_t \quad \text{Eq. 2}$$

where γ_d is the velocity gain signal that contributes to under-estimation or over-estimation of the linear velocity and ν_t as the Gaussian noise with mean zero and variance $\sigma_d^2|\delta_t|$ that increases proportionally with the magnitude of the linear velocity.

Table 1
Glossary of parameters used in the paper.

Observed or controlled by experimenter	
t	time step during translation
D_t	true distance at time t
α	true target distance
δ	true velocity
f	feedback distance
σ_f	standard deviation of true feedback
Observed, used, or computed by participant	
Estimates of distance	
m_t	estimated distance from path integration
s_t	uncertainty in path integration estimate of distance
s_0	subject's initial uncertainty in distance for path integration
$\widehat{m}_t$	estimated distance from Kalman filter
s_{t_f}	subject's uncertainty in distance at the end of feedback presentation in feedback trials
Estimates of task/subjects parameters	
s_X	subject's estimate of variability of the memory noise (i.e., their estimate of σ_X)
s_f	subject's estimate of variability of true feedback (i.e., subjects estimate of σ_f)
Parameters related to target distance	
X	subject's remembered target distance
β_X	subject's bias in remembered target distance
γ_X	subject's gain in remembered target distance
n_X	subject's noise in remembered target distance
σ_X	standard deviation of noise in subject's remembered target distance
Parameters related to velocity	
d	subject's estimate of velocity
γ_d	gain in subject's estimate of velocity
ν	noise in subject's estimate of velocity
σ_d	standard deviation of noise in subject's estimate of velocity

$$v \sim N\left(v_t|0,\sigma_d^2|\delta_t|\right) \quad \text{Eq. 3}$$

Next, we assume that participants integrate this noisy velocity estimate over time to compute an estimate of their distance. To perform this integration, we assume that participant's initial estimate of distance is centered at $D_0 = 0$ and their initial uncertainty in their distance is s_0^2

$$p(D_0) = N\left(D_0|0,s_0^2\right) \quad \text{Eq. 4}$$

Integrating the noisy velocity cues assuming a Gaussian probability distribution over their distance can be expressed as

$$\rho(D_t|d_{1:t-1}) = N\left(D_t|m_t, s_t^2\right) \quad \text{Eq. 5}$$

where m_t is the *participant's* estimate of the mean distance and s_t^2 corresponds to their uncertainty given by

$$m_t = \sum_{i=1}^{t} d_t = \gamma_d\delta_t + \sum_{i=1}^{t} v_t = \gamma_d\delta_t + n_d \quad \text{Eq. 6}$$

$$s_t^2 = s_0^2 + D_t s_d^2 \quad \text{Eq. 7}$$

where s_d^2 is the participant's estimate of the noise variance in their own vestibular system.

2.3.1.2. Target comparison. The second process involved in the path integration model is target comparison, where the noisy distance estimate is compared with the remembered target distance to produce a response. We assume that the participant's memory of the target distance X is an imperfect reflection of the true target α and can be scaled, noisy and biased

$$X = \gamma_X\alpha + \beta_X + n_X \quad \text{Eq. 8}$$

where γ_X and β_X are the gain and bias on participant's memory that leads to systematic over- or underestimation of the target distance, and n_X is zero-mean Gaussian noise with variance σ_X^2.

We assume that participants stop when their internal estimate of distance matches their internal estimate of the target; i.e., when

$$m_t = X \quad \text{Eq. 9}$$

Rearranging for the final, experimentally observed distance D_t, we get

$$D_t = \frac{1}{\gamma_d}(\gamma_X\alpha + \beta_X + n_X - n_d) \quad \text{Eq. 10}$$

Which allows us to write the distribution over the final *error* in the distance as a Gaussian with mean

$$E[D_t - \alpha] = \frac{(\gamma_X - \gamma_d)\alpha + \beta_X}{\gamma_d} \quad \text{Eq. 11}$$

and variance

$$V[D_t - \alpha] = \frac{\sigma_d^2\alpha + \sigma_X^2}{\gamma_d^2} \quad \text{Eq. 12}$$

This way the path integration model predicts a linear relation to the target distance, α, for both mean error and variance. In the Feedback condition, this model ignores the visual feedback and so predicts no relationship between feedback offset and response error (Fig. 3A).

2.3.2. Kalman filter model

The Kalman filter model, unlike the pure path integration model, combines the path integration estimate of location with an estimate based on visual feedback (Fig. 4). While the Kalman filter captures key features from a landmark navigation model, it is not a "pure" landmark navigation model which is also modelled in this study (described below). In the Kalman filter model, we assume participants integrate visual feedback such that when the visual feedback disappears, halfway to actual target, they update their distance estimate with the initial uncertainty estimate and feedback in a Bayesian manner. In this way, the Kalman filter model acts as a Bayesian cue combination model. Path integration velocity estimates during feedback presentation are assumed to be consistent with the visual input and hence the initial uncertainty is estimated at the end of feedback presentation.

The retrieval phase of the task is broken down into three stages in the Kalman filter model: feedback incorporation; path integration, after feedback is turned off; and target comparison, to determine the stop/response distance.

2.3.2.1. Feedback incorporation. The Kalman filter model combines the initial distance estimate at the end of feedback presentation, m_{t_f}, with the feedback, f, in a Bayesian manner under the assumption that both the feedback and initial distance estimate come from Gaussian distributions. Thus, as in the path integration model, this model assumes that the distribution over initial location is

$$p\left(D_{t_f}\right) = N\left(D_{t_f}\middle|m_{t_f}, s_{t_f}^2\right) \quad \text{Eq. 13}$$

where m_{t_f} is the mean of the subject's estimate and s_{t_f} is their uncertainty.

For feedback, the Kalman filter model assumes that the distribution over the feedback given the true location D_{t_f} is also a Gaussian

$$N\left(f|D_{t_f}, s_f^2\right) \quad \text{Eq. 14}$$

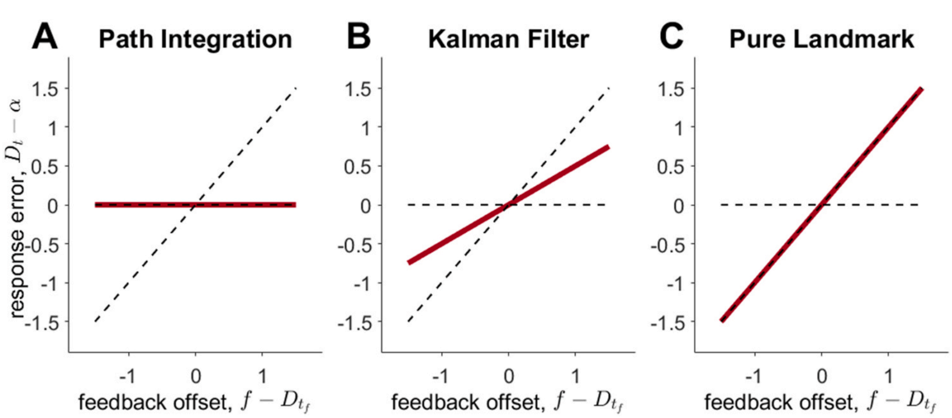

Fig. 3. Model prediction for path integration, Kalman filter, and pure landmark models. (A–C) Red lines show the mean of the response error prediction as a function of feedback offset by model using same fit parameters.

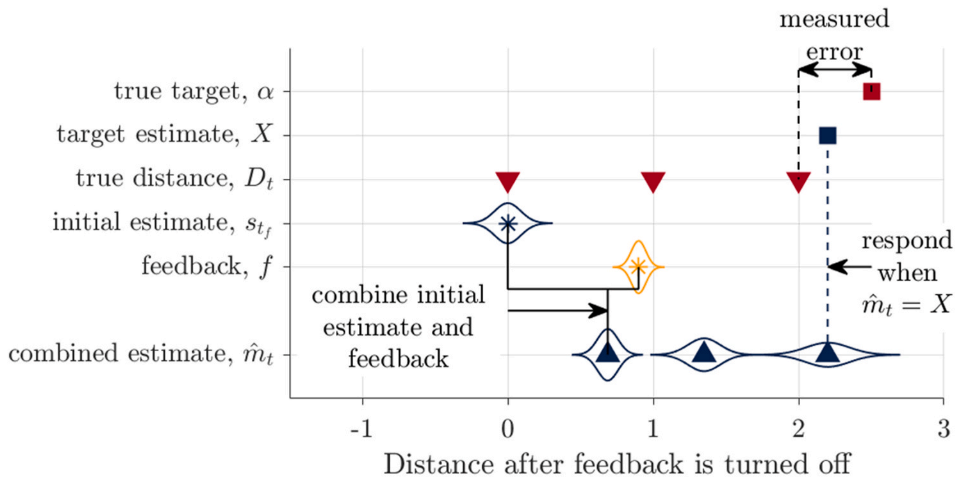

Fig. 4. Schematic of Kalman filter model. The Kalman filter model assumes that participants combine the feedback, f, with their initial uncertainty estimate, s_{t_f}, to compute a combined estimated over their heading, $\hat{m}_t$, once the feedback presentation ends. During feedback presentation, participant's velocity estimates are assumed to be consistent with the visual input. Participants stop walking and indicate their response when $\hat{m}_t = X$, their memory of the target. None of the internal variables (blue icons) are observed by the experimenter, and the response error is measured as the difference between true heading, D_t, and true target distance, α.

where subject's estimate of s_f^2 is the uncertainty in the feedback. Note that this *subjective* estimate of the distribution over the feedback is *not* the same as the true distribution over the feedback (given by Eq. (1)) which is non-Gaussian.

With these Gaussian assumptions, we assume that participants compute the posterior distribution over initial location as

$$\begin{aligned} p(D_{tf}|f) &= \overbrace{N\left(f|D_{tf}, s_f^2\right)}^{\text{feed back}} \times \overbrace{N\left(D_{tf}\middle|m_{tf}, s_{tf}^2\right)}^{\substack{\text{initial estimate}\\ \text{(end of feedback)}}} \\ &=> p(D_{tf}|f) = N\left(D_{tf}\middle|\hat{m}_{tf}, \hat{s}_{tf}^2\right) \end{aligned} \quad (15)$$

where $\hat{s}_{t_f}^2$ is the variance of the posterior and $\hat{m}_{t_f}$ is the mean of the posterior distribution given by

$$\hat{m}_{t_f} = m_{t_f} + K_{t_f}\left(f - m_{t_f}\right) \quad \text{Eq. 16}$$

where $K_{t_f} \in [0, 1]$ is the 'Kalman gain' given by

$$K_{t_f} = \frac{s_{t_f}^2}{s_f^2 + s_{t_f}^2} \quad \text{Eq. 17}$$

Kalman gain captures the relative weighting of visual feedback (allothetic) and initial uncertainty (idiothetic) in estimating distance. A Kalman gain value close to 0 is derived when the model relies more on initial distance, thus weighting more on the idiothetic cues. If the model believes that the visual feedback is more reliable, then Kalman gain is closer to 1 and the allocentric cue is weighted more heavily. It is important to note here that the path integration and pure landmark navigation models are extreme cases of the Kalman filter model, where the Kalman gain is 0 in the path integration model, ignoring visual feedback completely, and 1 in the pure landmark navigation model, incorporating visual feedback completely.

2.3.2.2. Path integration. After feedback presentation ends, the model continues to path integrate using noisy velocity information until this estimate of distance matches the memory of the target distance.

$$\hat{m}_t = \hat{m}_{t_f} + \sum_{i=t_f}^{t-1} d_i \quad \text{Eq. 18}$$

Substituting $\hat{m}_{t_f}$, d_i and m_{t_f} we get

$$\begin{aligned} \hat{m}_t &= m_{tf} + k_{tf}(f - m_{tf}) + \sum_{i=t_f}^{t-1}(\gamma_d\delta_i + v_i) \\ &= \sum_{i=1}^{t}(\gamma_d\delta_i + v_i) + K_{tf}\left(f - \sum_{i=1}^{t}(\gamma_d\delta_i + v_i)\right) + \sum_{i=t_f}^{t-1}(\gamma_d\delta_i + v_i) \\ &= \gamma_d D_t + K_{tf}(f - \gamma_d D_{tf}) + \underbrace{\sum_{i=1}^{t}(1 - k_{tf})v_i + \sum_{i=t_f}^{t-1} v_i}_{\text{noise},\epsilon} \end{aligned} \quad (19)$$

2.3.2.3. Target comparison. The response is determined as the point at which $\hat{m}_t$ is thought to be equal to the remembered target distance, X

$$\hat{m}_t = \gamma_X\alpha + \beta_X + n_X \quad \text{Eq. 20}$$

Substituting the expression for $\hat{m}_t$ and solving for the distance gives

$$D_t = \frac{1}{\gamma_d}\left(\gamma_X\alpha - K_{t_f}\left(f - \gamma_d D_{t_f}\right) + \beta_X + n_X - \epsilon\right) \quad \text{Eq. 21}$$

The response error is calculated assuming the measured response distribution is Gaussian with mean given by

$$E[D_t - \alpha] = \frac{1}{\gamma_d}\left((\gamma_X - \gamma_d)\alpha - K_{t_f}\left(f - \gamma_d D_{t_f}\right) + b\right) \quad \text{Eq. 22}$$

and variance given by

$$\begin{aligned} V[D_t - \alpha] &= \frac{1}{\gamma_d}\left(\sigma_X^2 + \left(1 - K_{t_f}\right)^2 K_{t_f} D_{t_f} + \left(\alpha - D_{t_f}\right)\sigma_d^2\right) \\ &= \frac{1}{\gamma_d}\left(\sigma_X^2 + \left(\alpha - \left(2 - K_{t_f}\right)K_{t_f}D_{t_f}\right)\sigma_d^2\right) \end{aligned} \quad \text{Eq. 23}$$

There are 7 free parameters in this model ($\gamma_d, \sigma_d, \gamma_X, \beta_X, \sigma_X, s_{t_f}, s_f$). However, because s_{t_f} and s_f only appear as a ratio in K_{t_f}, only one of the two can be estimated from the data. Thus, when fitting the Kalman filter model we set $s_f = 1$ and estimated initial uncertainty estimate as, s_{t_f}/s_f (Table 2). When simulated, the error in the Kalman filter model is linear in the feedback prediction error $f - \gamma_d D_{t_f}$ (Fig. 3B).

2.3.3. Pure landmark navigation model

The "pure" landmark navigation model has one key difference from the Kalman model we will describe shortly and that is that the Kalman

Table 2
Parameters estimated in each model and their ranges.

Parameter and range	Path integration	Kalman filter	Pure landmark navigation
Velocity gain, γ_d $0 \le \gamma_d \le 4$	$= 1$	✓	✓
Variance of velocity noise, σ_d^2 $0 \le \sigma_d \le 10$	σ_d/γ_d	✓	✓
Target gain, γ_X $0 \le \gamma_X \le 5$	γ_X/γ_d	✓	✓
Target bias, β_X $-10 \le \beta_X \le +10$	β_X/γ_d	✓	✓
Variance of target noise, σ_X^2 $0 \le \sigma_X \le 5$	σ_X/γ_d	✓	✓
Participant's initial uncertainty, $s_{t_f}^2$ $0 \le s_{t_f} \le 20$		s_{t_f}/s_f	
Participant's feedback noise variance, s_f^2 $0 \le s_f \le 20$		$= 1$	

gain is set to 1. This forces the model to base its estimate of distance entirely on the visual feedback and ignoring the initial uncertainty (idiothetic) estimate. This implies that the error in pure landmark navigation model is linear with response error matching feedback offset (Fig. 3C). Given that our initial observation clearly shows that many participants were incorporating the visual feedback, the pure landmark navigation model serves as a better comparison with the Kalman filter model.

2.4. Model fitting and comparison

The model fitting used in our experiment has been described in detail elsewhere (Harootonian et al., 2022). Briefly, the likelihood of a particular distance error on a trial, τ, given target and feedback (in feedback conditions) is provided by each model. The likelihood of observing error$^\tau$ on trial τ is given by

$$p(\text{error}^\tau|\text{X}) = \begin{cases} p(\text{error}^\tau|\alpha^\tau,\text{X}) & \text{No Feedback condition} \\ p\left(\text{error}^\tau\middle|\alpha^\tau, f^\tau, D_{t_f}^\tau, \text{X}\right) & \text{Feedback condition} \end{cases} \quad \text{Eq. 24}$$

where vector X denotes the free parameters of the model. The parameters were yoked with the path integration model and so all models had equal parameters for comparison across No Feedback and Feedback trials. Then, the log likelihood for a given set of parameters was computed for all trials. The best fit parameters were used to maximize the log likelihood. Model fitting was performed using the fmincon function in Matlab (R2024b) with 100 iterations of this process to reduce the local minima possibility with each parameter being randomly sampled between the lower and upper bounds (Table 2).

Model comparison was executed by computing the Bayes Information Criterion (BIC) for each participant and model given by

$$BIC = k \log n - 2LL(\text{X}_{MLE}) \quad \text{Eq. 25}$$

where k is the number of free parameters, n is the number of trials, LL is the log likelihood calculation and X_{MLE} is the maximized log likelihood.

2.5. Simulation

The simulated data was generated by simulating the models using the process described above. The best fit parameters from participants were randomly selected to generate simulated participant data to ensure a reasonable range of parameter values during simulation. Thus, for a given simulated participant data the parameter value for velocity gain could be from participant 3, and velocity noise from participant 15, and so on. This way, we simulated data for 30 participants for the three models (90 simulated participants in total) on the same (but scrambled) set of trials seen by participants in our task. The simulated data was then fit to the models to obtain best fitting parameters and the BIC scores for each. For parameter recovery analysis, the simulated data was fit with the same model and the resulting parameter estimates were correlated between the fit and simulation with higher correlation results indicating a better parameter recovery for a given model.

The BIC scores from the simulation were used to compute the 'confusion matrix' to determine model recovery, i.e. to determine whether model X is always best fit by model X. The BIC scores in the confusion matrix were expressed as the fraction of times the data generated by model X was best fit by model Y, $p(\text{fit} = Y \mid \text{sim} = X)$.

3. Results

3.1. Computational properties of the translation task

Before fitting our models to human data, we used simulations to test the validity of our model fitting procedures. For each model, we simulated behavior using parameters that were close to those ultimately found to fit human behavior. We then fit this simulated data to test both model recovery, i.e. whether the best-fitting model matched the data

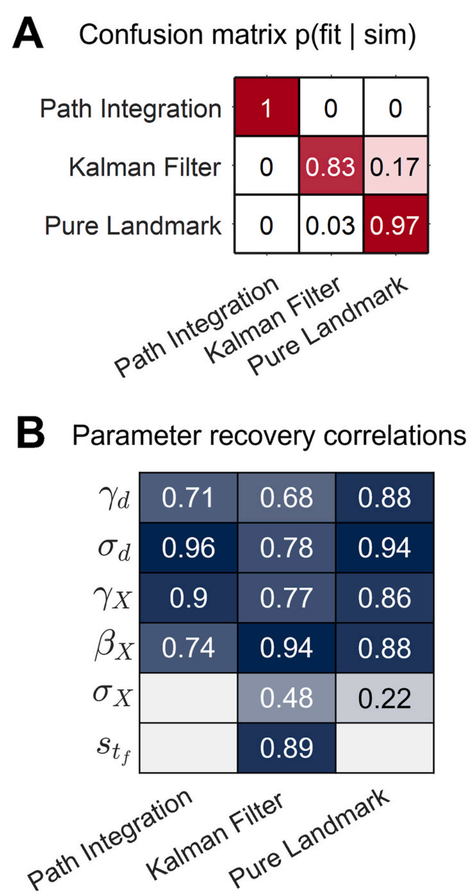

Fig. 5. Model recovery and parameter recovery: (A) Confusion matrix showing the frequency with which data generated according to each model is best fit by itself and by another model, ρ (fit model | simulated model). (B) Parameter recovery results as correlations (r values from Spearman correlation) between simulated and fit parameters estimated for each model. Numbers highlighted in white indicate significance, $p < 0.05$. Velocity gain, γ_d; Variance of velocity noise, σ_d; Target gain, γ_X; Target bias, β_X; Variance of target noise, σ_X; Participant's initial uncertainty, s_{t_f}

generating model, and parameter recovery, whether the best-fitting parameters matched the data generating parameters for each model.

Model recovery results are shown in the confusion matrix in Fig. 5A. The near diagonal form of this matrix demonstrates the task's good computational properties for distinguishing these three models. For the path integration and pure landmark navigation models, there is a near perfect relationship where >97 % of the data generated by either model is best fit by the respective models. For the Kalman filter model, 83 % of the time when data was generated from the Kalman filter model it was also best fit by the Kalman filter model. More broadly, the task is limited in its ability to distinguish between different types of cue integration models. Specifically, when we simulate data according to the cue combination and hybrid models described in our previous paper (Harootonian et al., 2022), these models, and a new random-sampling model, were indistinguishable from the Kalman Filter model (Supplementary Fig. 1). This was due to physical constraints from the size of the room that limit the maximum offset range to ± 1.5 meters. Indeed, when we simulate a task with a much larger offset we can better distinguish models (Supplementary Fig. 2). Thus, we conclude that our task and modeling approach can distinguish between pure path integration, pure landmark navigation and cue integration models, but not between different flavors of cue integration.

Parameter recovery results – in the form of correlations between simulated and fit parameters – are shown in Fig. 5B. Parameter recovery is good for almost all models with significant correlation between simulated and fit parameters. The one exception is the target noise parameter in the pure landmark model.

Taken together these simulations show that the Translation Task has good computational properties for distinguishing between three models and identifying their parameters.

3.2. Performance in the No feedback condition is consistent with path integration with a tendency to underestimate distance

The translation behavior during No Feedback trials serves as a check for participants' ability to reproduce distance estimates with just idiothetic body-based cues using path integration. The path integration model predicts a linear relationship between response error and target distance, α. This linear relationship is confirmed in Fig. 6. In line with our prediction, we saw a clear linear relationship between response error and target distance. In addition, variability in response error increased with longer target distances, which is consistent with noisy velocity parameter estimate in the path integration model. Interestingly, most participants had a negative slope, meaning that participants systematically underestimated the longer target distances. This could be due to leaky path integration estimates over longer distances, with error increasing monotonically as a function of distance (Harootonian et al., 2020; Petzschner and Glasauer, 2011). This underestimation effect could also be due to fear of walking into a wall.

To further characterize behavior on the No Feedback trials, we fit the path integration model. The model has 5 free parameters capturing the gain and noise in velocity (γ_d, σ_d) and the gain, noise and bias in the target distance encoding ($\gamma_X, \sigma_X, \beta_X$). However, because the velocity gain parameter, γ_d, only appears as a ratio in all the path integration equations, only the ratios of each parameter with velocity gain can be estimated from No Feedback behavior (Supplementary Fig. 3).

As shown in Fig. 6, the model provides a good fit to the data from all participants. Consistent with the negative slope in Fig. 6, the gain on target distance is below 1 for all participants (mean $\gamma_X/\gamma_d = 0.71$) suggesting a systematic underestimation of target location in participants. Consistent with the non-zero intercept, we see a target bias that is greater than 1 (mean $\beta_X/\gamma_d = 1.39$). Together these two effects are consistent with a regression to the mean effect, in which participants overestimate short distances and under estimate long distances (Fujita et al., 1993; Petzschner and Glasauer, 2011).

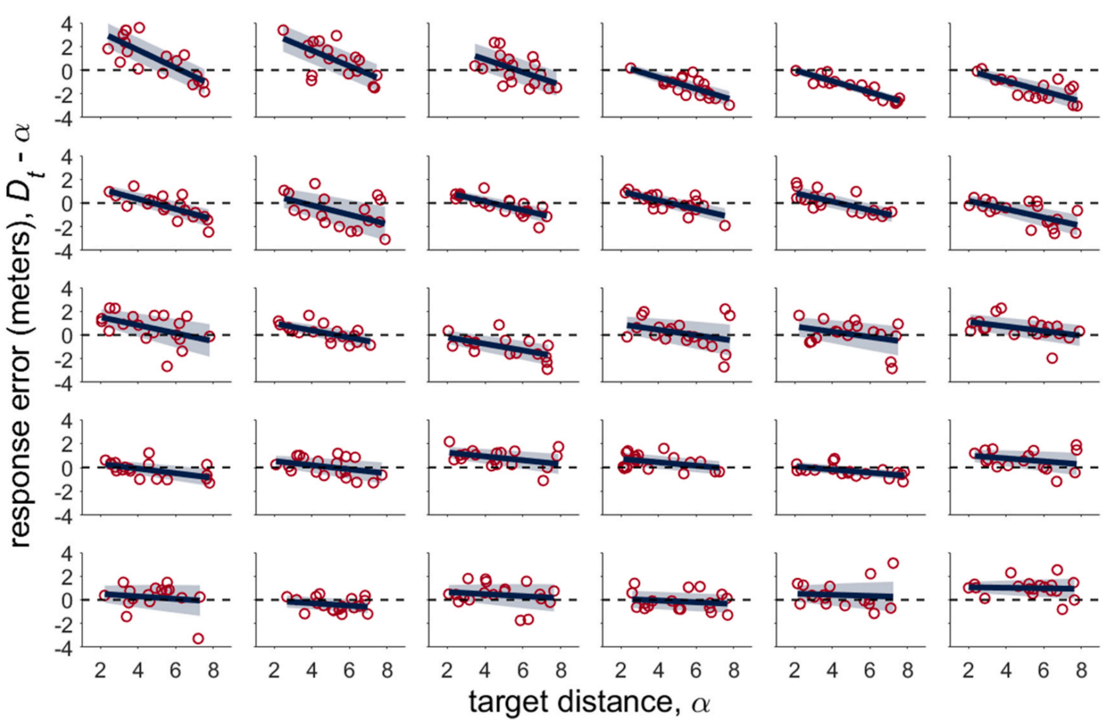

Fig. 6. Linear path integration during No Feedback trials. Scatter plots showing response error, $D_t - \alpha$, as a function of target angle, α, for No Feedback trials for each participant (n = 30) which are ordered by slope (negative to positive, left to right). The behavioral data is shown in red circles, the blue line corresponds to the mean response error from the path integration model, and the shaded blue area is the mean ± standard deviation of the response error from the path integration model fit.

Finally, we note that there is substantial variability in the parameters between people suggesting that there are considerable individual differences in path integration in the No Feedback condition.

3.3. Feedback incorporation for distance estimation is consistent with Bayesian cue combination

For the feedback condition, the relationship between feedback offset, $f - D_{t_f}$, and response error, $D_t - \alpha$, is key to assessing the effect of feedback on distance estimation. This is illustrated for all models in Fig. 3. We show a few examples of translation behavior qualitatively consistent with all three models (Fig. 7). Participant 25 seems to ignore visual feedback and suggests a reliance on path integration information. In contrast, participant 12 and 7 almost always incorporated feedback. Participant 7 showed almost pure dependence on landmark navigation and participant 12 appeared to employ cue integration.

The best fit model for a given participant was determined quantitatively by computing Bayes Information Criterion (BIC) scores. This measure penalizes the likelihood values of each model fit by the number of free parameters. The path integration, Kalman filter, and pure landmark models have 4, 6, and 5 free parameters respectively (Table 2), not counting the parameter expressed only as a ratio (γ_d) or set to 1 when fitting the model (s_f). The lowest BIC scores across the three models for all participants were calculated (Fig. 8). The total number of best fits for each model is shown in Fig. 8A. The BIC score relative to the Kalman filter model is shown in Fig. 8B, where negative values indicate a worse fit and positive values indicate a better fit to the Kalman filter model compared to either pure landmark or path integration models. Results from model fitting show that data favors the Kalman filter model and thus best describes this behavior in most participants (n = 24) in our experiment.

Qualitatively looking at the behavior of the Kalman filter model, it is evident that it provides a good account of data for most participants (Fig. 9). As suggested in Fig. 7, participant 12 was indeed best fit by the Kalman filter model. This model also captures different degrees of feedback incorporation ranging from almost a “pure” landmark navigation such as in participant 1 to a modest level of incorporation as seen in participant 22.

The best fitting parameters for the Kalman filter model are shown in Fig. 10. The velocity gain γ_d estimate from the model is < 1 (mean $\gamma_d = 0.88$) indicating some systematic underestimation of velocity across participants (Fig. 10A). Like in the path integration model for the No Feedback condition, the target gain was consistently below 1 across participants (mean $\gamma_X = 0.73$) from the Kalman filter model fit for Feedback and No Feedback trials (Fig. 10C). Target bias, β_X was also underestimated with averaged estimate <1 across participants (mean $\beta_X = 0.85$; Fig. 10D). Thus, we observed a systematic underestimation of gain on velocity and target estimates and in target bias. The noise parameters had relatively small velocity noise (mean $\sigma_d = 0.26$; Fig. 10B) and target noise (mean $\sigma_X = 0.14$; Fig. 10E) across participants.

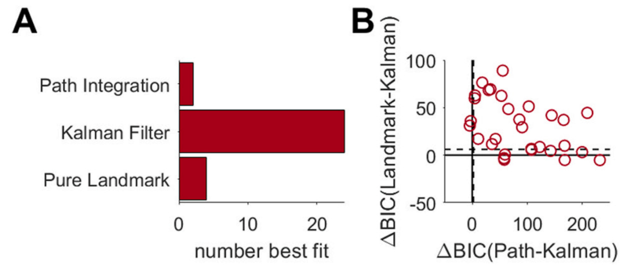

Fig. 8. Behavior data is best fit by the Kalman filter model. (A) The number of participants best fit by each model where 24 out of 30 participants were best fit by the Kalman filter model. (B) Bayes Information Criterion (BIC) scores for the path integration and pure landmark navigation model relative to the Kalman filter model with each circle corresponding to a participant. Positive values (top right quadrant) imply that the fit was better for the Kalman filter model and negative values imply that the fit favors the corresponding model on either axis. A Δ BIC value of >6 (dotted line) implies high posterior odds ($P(M_{Kalman}|Data) = 95-99\%$) (Raftery, 1995). https://doi.org/10.2307/271063

3.4. High inter-individual variability in feedback prediction error estimate of Kalman gain

Consistent with the behavior and Kalman filter parameter estimates, we saw substantial inter-individual differences in the values for Kalman gain (Fig. 11). As described in methods, the Kalman gain value is the key determinant for the weighting of allothetic visual feedback incorporation. While a small Kalman gain, close to 0, ignores visual feedback, a large Kalman gain value, closer to 1, favors visual feedback over idiothetic path integration estimates. We observed a full range of Kalman gain values from the Kalman filter model across participants (Fig. 11). Participants' behavior that best fit with the Kalman filter model (n = 24) show a substantial range of Kalman gain values ranging from 0.007 to 0.8. This almost uniform distribution of Kalman gain values indicates a high inter-individual variability in feedback incorporation based on prediction error estimation of distance.

4. Discussion

In our study, participants walked a variable distance in a straight-line while receiving visual feedback; they then attempted to reproduce the walked distance as closely as possible. In No Feedback trials,

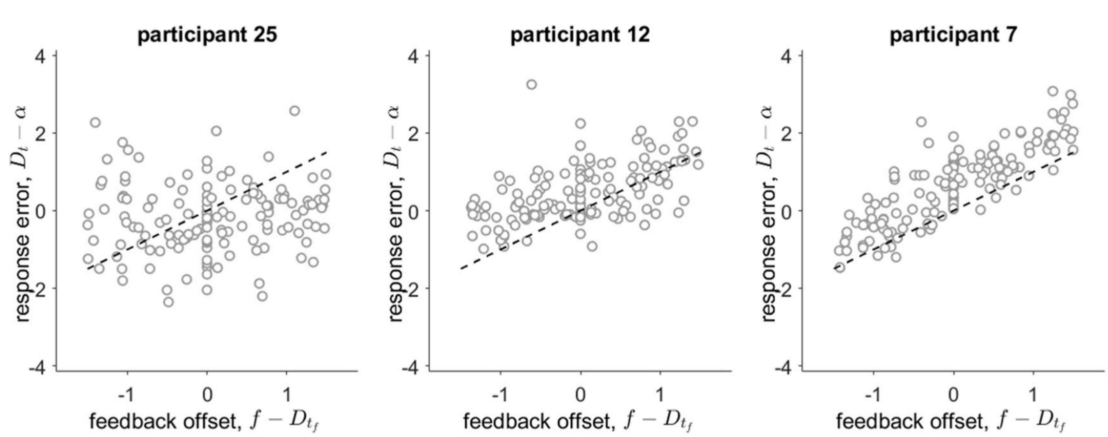

Fig. 7. Examples of participant behavior on feedback trials. Scatter plots show the response error, $D_t - \alpha$, as a function of feedback offset, $f - D_{t_f}$, for three representative participants.

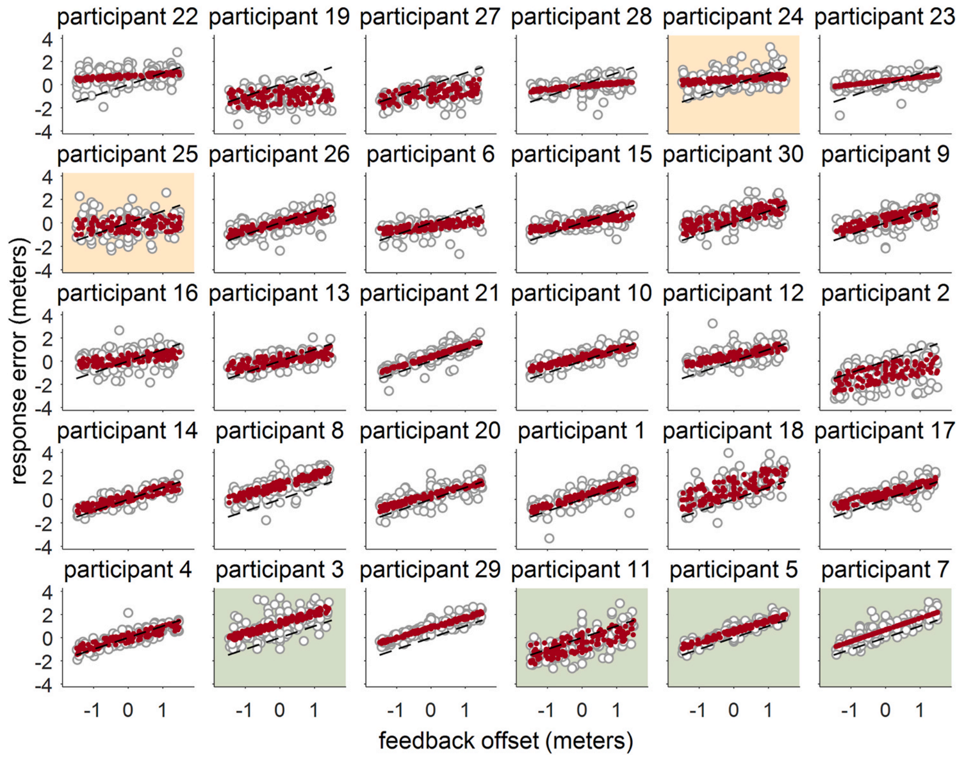

Fig. 9. Comparison between data and Kalman filter model for all participants. Scatter plots show the response error, $D_t - \alpha$, as a function of feedback offset, $f - D_{t_f}$, for each participant. The open grey dots correspond to the behavior data and the red dots are the mean response error from the Kalman filter model. The participants are ordered by Kalman gain going from lowest (top left) to highest (bottom right). The background color represents the best fit model: Kalman filter model (white), path integration (yellow), and pure landmark navigation model (green).

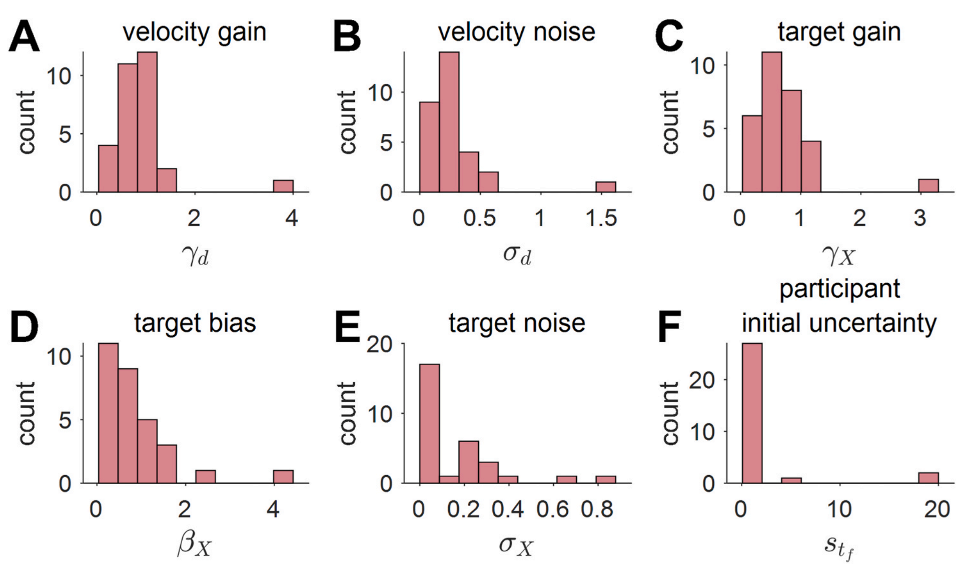

Fig. 10. Best fit parameters for the Kalman filter model. Histograms show the distribution of parameter values across participants (n = 30).

participants received no visual feedback during reproduction. In the Feedback condition, we manipulated visual landmarks where participants received potentially offset visual feedback at the start of reproduction.

In the No Feedback condition, it was clear that participants estimated the walked distance fairly accurately, although we did find some evidence for underestimation of distance. Our findings are consistent with previous work, where underestimation of walked distances has been observed in several different contexts of measurement of path integration, including the triangle completion task (Chrastil and Warren, 2021; Fujita et al., 1993; Harootonian et al., 2020; Klatzky, 1998). There has been evidence in prior path integration studies of this systematic underestimation due to leaky path integration (Harootonian et al., 2020) and regression to the mean and prior effects (Fujita et al., 1993; Petzschner and Glasauer, 2011). The behavior and prior knowledge from preceding trials was not accounted for in modelling distance error estimates. A study by Petzschner and Glasauer (2011), did model prior knowledge in a desktop version of isolated distance estimation task where they found a regression to the mean and range effect in distance estimation. In future studies, given the systematic errors, it would be

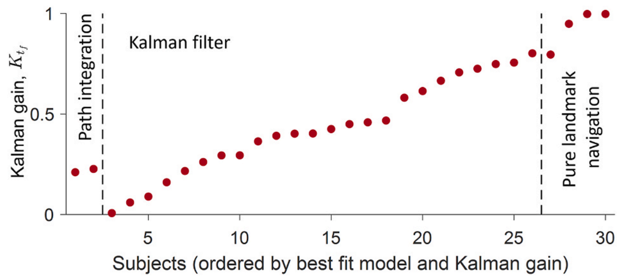

Fig. 11. Kalman gain values computed for each participant. The Kalman gains computed for all participants ordered by best fit model and lowest to highest Kalman gain within each model.

crucial to add prior knowledge effects when investigating strategy differences involved in integrating path integration and misleading visual landmarks.

In our Feedback condition, we found evidence for individual differences amongst participants, although the majority of participants showed evidence for Bayesian integration. We found that a small subset of participants (n = 2) largely ignored the translated room and instead reproduced the encoded distance based on path integration. We term this subset of participants "path integrators" as they relied primarily on idiothetic information. Another small subset of participants (n = 4) relied only on the visual feedback (i.e., the moved room) to reproduce the encoded distance. These participants could be considered "landmark integrators" and largely relied on the available allothetic information.

Most participants (n = 24), however, used a Bayesian cue combination strategy in which they sometimes incorporated misleading visual information with their path integration estimates, with the extent of incorporating it depending on their perceived level of uncertainty. These participants, who were best modelled by a Kalman filter model, employed path integration and visual feedback to different degrees depending on their internal estimates. We found a full range of feedback incorporation in these participants, where some participants consistently held higher uncertainty for visual feedback thus incorporating visual feedback but weighting more heavily on their path integration estimate (Kalman gain close to 0). While some participants weighted the uncertainty almost equally between visual feedback and path integration estimates (Kalman gain close to 0.5). Yet another set of participants consistently held higher uncertainty in their path integration estimate and relied more heavily on the visual feedback (Kalman gain close to 1). Thus, this set of important results from our experiment suggest individual differences in how idiothetic and allothetic information is integrated and incorporated, consistent with other studies suggesting that navigation often involves different strategy combinations across participants (Ishikawa and Montello, 2006; Weisberg et al., 2014).

This special issue focuses on the idea of maps in the brain. Presumably, participants formed some kind of representation when they first encoded the room environment, although our study did not involve specific tests to determine whether this had a map-like structure (i.e., Euclidean or non-Euclidean). When participants retrieved this representation initially after turning around they used this to plan their trajectory. What is striking is that a large number of participants altered how far they walked based on the initial misleading visual feedback. This suggests that the representation they had formed during encoding was malleable and subject to potential overwriting from allothetic cues. This conflicts somewhat with the classic view of the cognitive map in that path integration information should be primary; instead, in many cases, the representation was altered or perhaps even overwritten by visual information even during uncertainty.

What might have driven the different levels of uncertainty in participants to decide whether to incorporate the visual feedback? Past studies have suggested that combining different cues in experiments involving more complicated paths could involve an optimized process in which the uncertainty in each estimate is minimized (Chen et al., 2017; Nardini et al., 2008; Whishaw and Tomie, 1997; Xu et al., 2017). Our findings are broadly consistent with this perspective in that most participants used both path integration and visual feedback in some form to estimate distance. Our findings of significant individual variability are not consistent with an account, however, in which cue combination is optimal across participants. In a past study, we found evidence that participants incorporated misleading visual feedback during reproduction of rotations but that participants combined feedback when the change in visual feedback was small and relied on path integration when change in visual feedback was large using a "sampling" (hybrid) strategy (Harootonian et al., 2022). We tested similar models in this paper (cue combination/averaging and hybrid, both of which can be considered extensions of the Kalman model) and neither showed a better fit for the data than the Kalman model, i.e. Bayesian cue combination. These findings would suggest that participants incorporate feedback but the extent to which they do can be attributed to the degree of mismatch between encoding and retrieval. Although we do not know the exact reasons in this study that lead to either incorporation or ignoring of the visual feedback, we think it is likely that prior trials and levels of mismatch played some role, as was reported in a previous paper on the triangle completion task (Harootonian et al., 2020).

One limitation of the study that could also explain why we did not see evidence for cue incorporation based on the degree of mismatch is that the range of visual feedback length we used for translation was relatively small, ± 1.5 m. While in our previous Rotation Task, where we did see evidence for a hybrid strategy, we were able to employ a large, $\pm 180^{\circ}$, range of mismatched visual feedback. We initially piloted the current study in a smaller room with a shorter range of distances and were not successful in getting participants to incorporate misleading visual feedback. Although the range we used for translation was sufficient to induce uncertainty in path integration estimates, this more limited range did limit the extent to which we could model trials in which the visual feedback was completely ignored. This limitation, however, is of universal consideration in most immersive virtual reality experiments where physical space dictates the extent and feasibility of experimental design. Also, it is still possible that translation, even at longer distances, is simply less susceptible to overriding with visual information than rotations.

It is important to note that translation and rotation differ from each other based on the nature of the idiothetic cues. Translation depends largely on acceleration signals from the otoliths (Green et al., 2005), proprioceptive information from shuffling and moving the feet, and motor efference copy from stride movements (Angelaki and Cullen, 2008). In contrast, rotations likely depend on somewhat different inputs, including rotational acceleration from the semi-circular canals (Angelaki et al., 1995), foot turns, and motor efference copy from hip rotations (Angelaki and Cullen, 2008; Kleine et al., 2004). As such, the nature of the inputs between the two different tasks likely differs substantially. As one line of evidence for the importance of the difference in inputs, we found that participants incorporated misleading visual input even when it was just a brief flash in the Rotation Task. In contrast, during the initial pilot of our task, not reported here, we found that a brief flash during translation was insufficient to override path integration. In fact, the room had to be present for the first half of the trial to see any effects on participant errors due to the mismatching visual information. This suggests that translation may be less sensitive to misleading visual information. This could be due to differences in the sensory input and/or one's everyday experience with translation compared to rotation.

In conclusion, we found that majority of participants in this study conformed to a Bayesian cue combination strategy to reconcile mismatched visual landmarks with their body-based estimates of straight-line distance. We also found, based on our previous work on angular estimation, that distance and angular estimations might employ different cue integration strategies. It would be prudent to test in future studies if there are within subject strategy disparities between these fundamental spatial estimates involved in navigation and the neural correlates associated with these approaches to behavior.

CRediT authorship contribution statement

Abhilasha Vishwanath: Writing – review & editing, Writing – original draft, Visualization, Validation, Software, Project administration, Methodology, Investigation, Formal analysis, Data curation. **Matthew F. Watson:** Validation, Software, Project administration, Methodology. **Melanie K. Gin:** Validation, Software. **Donnette C. Markham:** Project administration, Data curation. **Yinqi Huang:** Methodology, Funding acquisition. **Yu K. Du:** Software, Methodology. **Arne Ekstrom:** Writing – review & editing, Visualization, Validation, Supervision, Software, Resources, Project administration, Methodology, Investigation, Funding acquisition, Conceptualization. **Robert C. Wilson:** Writing – review & editing, Visualization, Validation, Supervision, Software, Resources, Project administration, Methodology, Investigation, Funding acquisition, Formal analysis, Conceptualization.

Author disclosure

The authors have no competing interests to disclose.

Funding

This work was funded by NIH/NIMH R21 MH134100 to RCW and AE and a grant from The University of Arizona Sensor Lab.

Appendix A. Supplementary data

Supplementary data to this article can be found online at https://doi.org/10.1016/j.neuropsychologia.2025.109351.

Data availability

TranslationModeling (Original data) (GitHub)

References

Angelaki, D.E., Cullen, K.E., 2008. Vestibular system: the many facets of a multimodal sense. Annu. Rev. Neurosci. 31, 125–150. https://doi.org/10.1146/annurev.neuro.31.060407.125555.

Angelaki, D.E., Hess, B.J., Suzuki, J., 1995. Differential processing of semicircular canal signals in the vestibulo- ocular reflex. J. Neurosci. 15 (11), 7201–7216. https://doi.org/10.1523/JNEUROSCI.15-11-07201.1995.

Chen, X., McNamara, T.P., Kelly, J.W., Wolbers, T., 2017. Cue combination in human spatial navigation. Cognit. Psychol. 95, 105–144. https://doi.org/10.1016/j.cogpsych.2017.04.003.

Chen, X., Chen, Y., McNamara, T.P., 2025. Processing spatial cue conflict in navigation: distance estimation. Cogn. Psychol. 158, 101734. https://doi.org/10.1016/j.cogpsych.2025.101734.

Chrastil, E.R., Sherrill, K.R., Aselcioglu, I., Hasselmo, M.E., Stern, C.E., 2017. Individual differences in human path integration abilities correlate with gray matter volume in retrosplenial cortex, hippocampus, and medial prefrontal cortex. eNeuro 4 (2). https://doi.org/10.1523/ENEURO.0346-16.2017.

Chrastil, E.R., Warren, W.H., 2021. Executing the homebound path is a major source of error in homing by path integration. J. Exp. Psychol. Hum. Percept. Perform. 47 (1), 13–35. https://doi.org/10.1037/xhp0000875.

Deery, R., Commins, S., 2023. Landmark distance impacts the overshadowing effect in spatial learning using a virtual water maze task with healthy adults. Brain Sci. 13 (9), 1287. https://doi.org/10.3390/brainsci13091287.

Deneve, S., Pouget, A., 2004. Bayesian multisensory integration and cross-modal spatial links. J. Physiol. Paris 98 (1), 249–258. https://doi.org/10.1016/j.jphysparis.2004.03.011.

Ehinger, B.V., Fischer, P., Gert, A.L., Kaufhold, L., Weber, F., Pipa, G., König, P., 2014. Kinesthetic and vestibular information modulate alpha activity during spatial navigation: a mobile EEG study. Front. Hum. Neurosci. 8, 71. https://doi.org/10.3389/fnhum.2014.00071.

Fujita, N., Klatzky, R.L., Loomis, J.M., Golledge, R.G., 1993. The encoding-error model of pathway completion without vision. Geogr. Anal. 25 (4), 295–314. https://doi.org/10.1111/j.1538-4632.1993.tb00300.x.

Green, A.M., Shaikh, A.G., Angelaki, D.E., 2005. Sensory vestibular contributions to constructing internal models of self-motion. J. Neural. Eng. 2 (3), S164. https://doi.org/10.1088/1741-2560/2/3/S02.

Harootonian, S.K., Ekstrom, A.D., Wilson, R.C., 2022. Combination and competition between path integration and landmark navigation in the estimation of heading direction. PLoS Comput. Biol. 18 (2), e1009222. https://doi.org/10.1371/journal.pcbi.1009222.

Harootonian, S.K., Wilson, R.C., Hejtmánek, L., Ziskin, E.M., Ekstrom, A.D., 2020. Path integration in large-scale space and with novel geometries: comparing vector addition and encoding-error models. PLoS Comput. Biol. 16 (5), e1007489. https://doi.org/10.1371/journal.pcbi.1007489.

Huffman, D.J., Ekstrom, A.D., 2019. A modality-independent network underlies the retrieval of large-scale spatial environments in the human brain. Neuron 104 (3), 611–622.e7. https://doi.org/10.1016/j.neuron.2019.08.012.

Ishikawa, T., Montello, D.R., 2006. Spatial knowledge acquisition from direct experience in the environment: individual differences in the development of metric knowledge and the integration of separately learned places. Cogn. Psychol. 52 (2), 93–129. https://doi.org/10.1016/j.cogpsych.2005.08.003.

Kessler, F., Frankenstein, J., Rothkopf, C.A., 2024. Human navigation strategies and their errors result from dynamic interactions of spatial uncertainties. Nat. Commun. 15 (1), 5677. https://doi.org/10.1038/s41467-024-49722-y.

Klatzky, R.L., 1998. Allocentric and egocentric spatial representations: definitions, distinctions, and interconnections. In: Freksa, C., Habel, C., Wender, K.F. (Eds.), Spatial Cognition: an Interdisciplinary Approach to Representing and Processing Spatial Knowledge. Springer, pp. 1–17. https://doi.org/10.1007/3-540-69342-4_1.

Kleine, J.F., Guan, Y., Kipiani, E., Glonti, L., Hoshi, M., Büttner, U., 2004. Trunk position influences vestibular responses of fastigial nucleus neurons in the alert monkey. J. Neurophysiol. 91 (5), 2090–2100. https://doi.org/10.1152/jn.00849.2003.

Knill, D.C., Pouget, A., 2004. The Bayesian brain: the role of uncertainty in neural coding and computation. Trends Neurosci. 27 (12), 712–719. https://doi.org/10.1016/j.tins.2004.10.007.

Ma, W.J., 2012. Organizing probabilistic models of perception. Trends Cognit. Sci. 16 (10), 511–518. https://doi.org/10.1016/j.tics.2012.08.010.

McNamara, T.P., Chen, X., 2022. Bayesian decision theory and navigation. Psychon. Bull. Rev. 29 (3), 721–752. https://doi.org/10.3758/s13423-021-01988-9.

Mou, W., Zhang, L., 2014. Dissociating position and heading estimations: rotated visual orientation cues perceived after walking reset headings but not positions. Cognition 133 (3), 553–571. https://doi.org/10.1016/j.cognition.2014.08.010.

Nardini, M., Jones, P., Bedford, R., Braddick, O., 2008. Development of cue integration in human navigation. Curr. Biol. 18 (9), 689–693. https://doi.org/10.1016/j.cub.2008.04.021.

Petzschner, F.H., Glasauer, S., 2011. Iterative Bayesian estimation as an explanation for range and regression effects: a study on human path integration. J. Neurosci. 31 (47), 17220–17229. https://doi.org/10.1523/JNEUROSCI.2028-11.2011.

Scherer, J., Müller, M.M., Unterbrink, P., Meier, S., Egelhaaf, M., Bertrand, O.J.N., Boeddeker, N., 2024. Not seeing the forest for the trees: combination of path integration and landmark cues in human virtual navigation. Front. Behav. Neurosci. 18. https://doi.org/10.3389/fnbeh.2024.1399716.

Schwartz, M., 1999. Haptic perception of the distance walked when blindfolded. J. Exp. Psychol. Hum. Percept. Perform. 25 (3), 852–865. https://doi.org/10.1037//0096-1523.25.3.852.

Singapogu, R.B., Sander, S.T., Burg, T.C., Cobb, W.S., 2008. Comparative study of haptic training versus visual training for kinesthetic navigation tasks. Medicine Meets Virtual Reality 16, 469–471. IOS Press. https://ebooks.iospress.nl/publication/11383.

Sjolund, L.A., Kelly, J.W., McNamara, T.P., 2018. Optimal combination of environmental cues and path integration during navigation. Mem. Cognit. 46 (1), 89–99. https://doi.org/10.3758/s13421-017-0747-7.

Starrett, M.J., McAvan, A.S., Huffman, D.J., Stokes, J.D., Kyle, C.T., Smuda, D.N., Kolarik, B.S., Laczko, J., Ekstrom, A.D., 2021. Landmarks: a solution for spatial navigation and memory experiments in virtual reality. Behav. Res. Methods 53 (3), 1046–1059. https://doi.org/10.3758/s13428-020-01481-6.

Teghtsoonian, R., Teghtsoonian, M., 1978. Range and regression effects in magnitude scaling. Percept. Psychophys. 24 (4), 305–314. https://doi.org/10.3758/BF03204247.

Waller, D., 2000. Individual differences in spatial learning from computer-simulated environments. J. Exp. Psychol. Appl. 6 (4), 307–321. https://doi.org/10.1037//1076-898x.6.4.307.

Waller, D., Nadel, L. (Eds.), 2013. Handbook of Spatial Cognition. American Psychological Association. https://doi.org/10.1037/13936-000.

Weisberg, S.M., Newcombe, N.S., 2018. Cognitive maps: some people make them, some people struggle. Curr. Dir. Psychol. Sci. 27 (4), 220–226. https://doi.org/10.1177/0963721417744521.

Weisberg, S.M., Schinazi, V.R., Newcombe, N.S., Shipley, T.F., Epstein, R.A., 2014. Variations in cognitive maps: understanding individual differences in navigation.

J. Exp. Psychol. Learn. Mem. Cognit. 40 (3), 669–682. https://doi.org/10.1037/a0035261.

Whishaw, I.Q., Tomie, J.-A., 1997. Piloting and dead reckoning dissociated by fimbria-fornix lesions in a rat food carrying task. Behav. Brain Res. 89 (1), 87–97. https://doi.org/10.1016/S0166-4328(97)00068-5.

Xu, Y., Regier, T., Newcombe, N.S., 2017. An adaptive cue combination model of human spatial reorientation. Cognition 163, 56–66. https://doi.org/10.1016/j.cognition.2017.02.016.

Zhao, M., Warren, W.H., 2015. How you get there from here: interaction of visual landmarks and path integration in human navigation. Psychol. Sci. 26 (6), 915–924. https://doi.org/10.1177/0956797615574952.

Further reading

Raftery, A.E., 1995. Bayesian Model Selection in Social Research. Sociol. Methodol. 25, 111–163. https://doi.org/10.2307/271063.